

## ORIGINAL ARTICLE

## ZNF750 is a lineage-specific tumour suppressor in squamous cell carcinoma

M Hazawa<sup>1,2,6</sup>, D-C Lin<sup>1,3,6</sup>, H Handral<sup>4</sup>, L Xu<sup>1</sup>, Y Chen<sup>1</sup>, Y-Y Jiang<sup>1</sup>, A Mayakonda<sup>1</sup>, L-W Ding<sup>1</sup>, X Meng<sup>1</sup>, A Sharma<sup>1</sup>, S Samuel<sup>1</sup>, MM Movahednia<sup>4</sup>, RW Wong<sup>2</sup>, H Yang<sup>1</sup>, C Tong<sup>4</sup> and HP Koeffler<sup>1,3,5</sup>

ZNF750 controls epithelial homeostasis by regulating epidermal-differentiation genes, a role underscored by its pathogenic mutations in esophageal squamous cell cancers (SCCs). However, the precise role of ZNF750 in SCC cell biology remains unclear. In this study, we report that ZNF750 is exclusively deleted, mutated and underexpressed in human SCCs, and low ZNF750 expression is associated with poor survival. Restoration of wildtype, but not mutant ZNF750 protein uniquely inhibited the malignant phenotypes of SCC cells both *in vitro* and *in vivo*. Notably, ZNF750 promoted the expression of a long non-coding RNA (TINCR), which mediated both cancer-inhibition and differentiation-induction effects of ZNF750. In addition, ZNF750 potently suppressed cell migration by directly inhibiting the transactivation of LAMC2. Together, our findings characterize ZNF750 as a crucial SCC-specific suppressor and uncover its novel anticancer-associated functions.

Oncogene (2017) 36, 2243–2254; doi:10.1038/onc.2016.377; published online 7 November 2016

## INTRODUCTION

Squamous cell carcinoma (SCC) is the most common human cancer. It arises from stratified epithelia, including the oral epithelium, epidermis and the epithelia covering the oesophagus, bladder, vulva and cervix. Approximately 300 000 new SCC cases per year occur in the United States alone, resulting annually in ~100 000 deaths.<sup>1,2</sup>

Recently, we and others identified missense and truncating mutations as well as genomic deletions targeting *ZNF750* in esophageal SCC (ESCC).<sup>3,4</sup> Functionally, we have shown that loss of *ZNF750* was associated with impaired differentiation as well as a failure to repress tumour growth in ESCC,<sup>3</sup> suggesting that *ZNF750* may act as a tumour suppressor. *ZNF750* was reported to function as a transcriptional regulator of epidermal cell differentiation by inducing differentiation genes while inhibiting progenitor factors.<sup>5</sup> However, the precise role of *ZNF750* in SCC cells largely remain unexplored. Particularly, the molecular events and signalling pathways associated with *ZNF750* in SCCs await further characterization.

Long non-coding RNAs (lncRNAs) have recently been reported to participate in the regulation of epidermal cell differentiation. For example, the lncRNA TINCR promotes differentiation of keratinocytes through a mechanism involving direct RNA:RNA interactions and recruitment of STAU1 protein to stabilize differentiation-specific mRNAs.<sup>6</sup> Another recent report demonstrated lncRNA/transcription factor network, which regulated epidermal differentiation.<sup>7</sup> However, whether and how these differentiation-associated lncRNAs are involved in the biology of SCC cells have not been fully addressed.

In this study, we demonstrate that *ZNF750* is frequently and exclusively targeted by genetic lesions in major types of human SCCs, including those cancers of the cervix (CSCC), head and neck (HNSCC) and lung (LSCC). Low expression level of *ZNF750* is

associated with poor prognosis of SCC patients. Furthermore, the tumour-suppressive role of *ZNF750* is mediated through regulating key cancer genes such as TINCR and LAMC2.

## RESULTS

*ZNF750* is exclusively mutated, deleted and under-expressed in different types of human SCCs

To determine comprehensively the genetic abnormalities affecting *ZNF750*, multiple public datasets were re-analysed, including The Cancer Genome Atlas (TCGA), Gene Expression Omnibus (GEO) and Human Protein Atlas (see Materials and Methods). In TCGA whole-exome sequencing results, similar to our earlier findings in ESCC,<sup>3</sup> a number of mutations throughout *ZNF750* were identified in various SCC types, including CSCC, HNSCC and LSCC (Figure 1a). Of note, most of these somatic variants occurred at the beginning of Exon 2, which encodes for the evolutionally conserved C2H2 DNA-binding domain, highlighting the biologic relevance of this domain in SCC cells (Figure 1a). In addition, many of the mutations caused damaging effects to the *ZNF750* protein (for example, Stopgain, Frameshift and Splicing mutations). We next compared *ZNF750* gene dosage between tumour and normal samples using SNP 6.0 array data from TCGA, and found significant genomic deletions of *ZNF750* in primary SCC samples from cervical, head and neck, and lung tissues (Figure 1c). Importantly, these genetic abnormalities were exclusively observed in squamous-type tumours (Figure 1c), underscoring the lineage-specific role of *ZNF750* in squamous cancer biology.

Next, in order to examine *ZNF750* expression across different types of normal and cancer tissues at both mRNA and protein levels, we queried GEO cDNA microarray data (series GSE7307),

<sup>1</sup>Cancer Science Institute of Singapore, National University of Singapore, Singapore; <sup>2</sup>Cell-Bionomics Research Unit, Innovative Integrated Bio-Research Core, Institute for Frontier Science Initiative, Kanazawa University, Kanazawa, Japan; <sup>3</sup>Division of Hematology/Oncology, Cedars-Sinai Medical Center, University of California, Los Angeles School of Medicine, Los Angeles, California, USA; <sup>4</sup>Department of Oral and Maxillofacial Surgery, Faculty of Dentistry, National University of Singapore, Singapore and <sup>5</sup>National University Cancer Institute, National University Health System and National University of Singapore, Singapore. Correspondence: Dr M Hazawa, Institute for Frontier Science Initiative, Kanazawa University, Kanazawa 920-1192, Ishikawa, Japan or Dr D-C Lin, Los Angeles School of Medicine, Los Angeles, California 90048, USA  
E-mail: masaharu.akj@gmail.com or dchlin11@gmail.com

<sup>6</sup>These authors contributed equally to this work.

Received 28 February 2016; revised 25 August 2016; accepted 31 August 2016; published online 7 November 2016

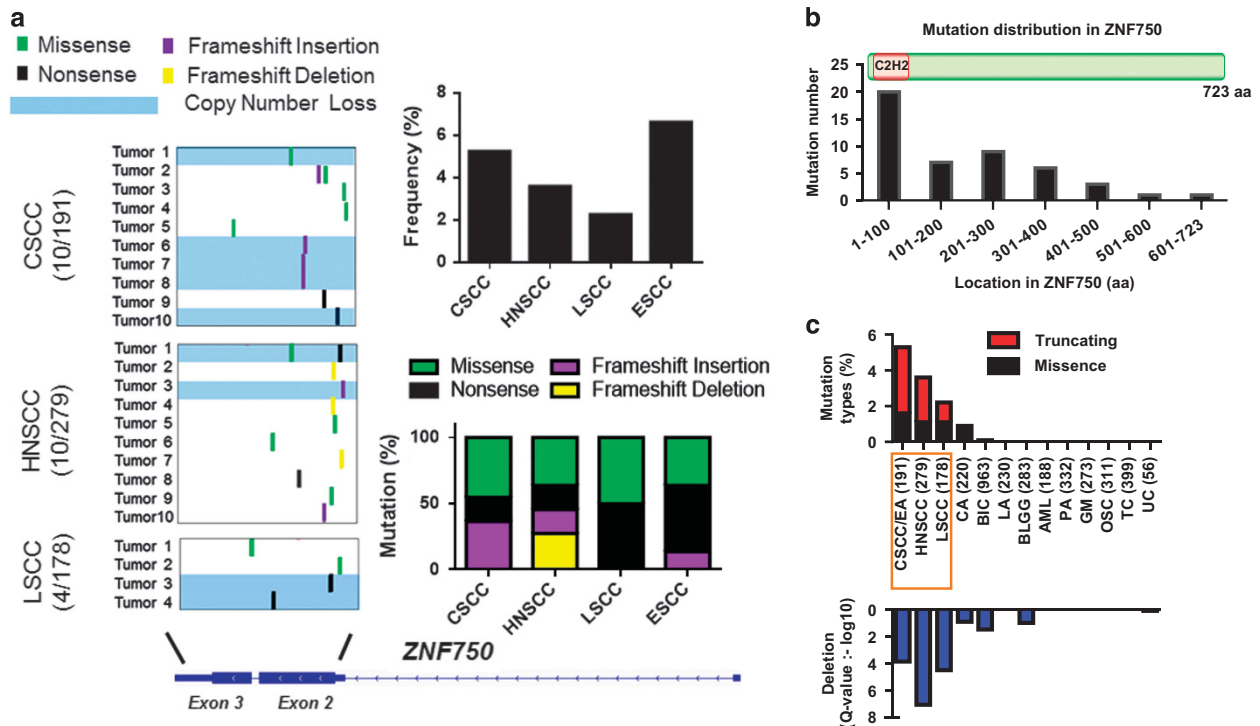


**Figure 1.** ZNF750 is exclusively disrupted in squamous cell carcinomas. (a) Analysis of ZNF750 somatic mutations in CSCC, HNSCC, LSCC from TCGA (see URL). Results in ESCC were summarized from published studies.<sup>3,4</sup> Different types of mutations and their location and frequency are shown. (b) Location of ZNF750 mutations in CSCC, HNSCC, LSCC and ESCC. (c) Summary of ZNF750 mutations across different tumour types from TCGA. Numbers in the parentheses indicate the number of cases sequenced. CSCC/EA, CSCC and endocervical adenocarcinoma; CA, colorectal adenocarcinoma; BIC, breast invasive carcinoma; LA, lung adenocarcinoma; BLGG, brain lower grade glioma; AML, acute myeloid leukemia; PA, prostate adenocarcinoma; GM, glioblastoma multiforme; OSC, ovarian serous cystadenocarcinoma; TC, thyroid carcinoma; UC, uterine carcinosarcoma.

TCGA RNA-seq data, as well as immunohistochemistry (IHC) results from Human Protein Atlas (see Materials and Methods). Notably, expression of both ZNF750 mRNA and protein was markedly higher in a variety of healthy squamous epithelium than non-squamous tissues, again signifying its lineage-specific expression pattern and function (Figures 2a and b). Moreover, results from GEO (series GSE9750 and GSE25099) and Human Protein Atlas showed significantly decreased ZNF750 expression compared to its normal counterpart at both mRNA (Supplementary Figure 1) and protein levels (Figure 2c) in CSCC and HNSCC. Congruent with these publically available data, we performed IHC analysis to stain samples from CSCC, HNSCC and LSCC (commercial tissue array, see Materials and Methods), and confirmed either lower or undetectable ZNF750 expression in tumour tissues (Figure 2d). Notably, Kaplan–Meier analysis on the TCGA cohorts revealed that the downregulation of ZNF750 was significantly correlated with poorer outcome of patients with HNSCC and LSCC (Log-rank test,  $P=0.04$  and  $0.01$ , respectively, Figure 2e). Collectively, these findings suggest that ZNF750 is uniquely compromised by multiple forms of genomic defects in human SCCs.

As a p63-dependent transcription factor, ZNF750 regulates KLF4 expression in SCC cells

ZNF750 was recently identified as a p63-downstream transcription factor, and activated KLF4 transcription in normal keratinocyte;<sup>5</sup> however, these regulations in the context of cancer cells are unknown. In order to investigate these transcriptional regulations in SCCs, we first depleted p63 using shRNA and confirmed that ZNF750 expression was decreased at both the mRNA and protein levels as addressed by qRT-PCR and western blot analysis

(Figures 3a and b). We next analysed p63 and ZNF750 protein levels in a panel of different types of SCC cell lines (Figure 3c). The abundance of p63 protein tended to have positive correlation with that of ZNF750 in 10 SCC cell lines tested (Figure 3d). Concordantly, analysis of 86 squamous cancer cell lines in Cancer Cell Line Encyclopedia (CCLE) datasets showed a significant linear correlation between the mRNA levels of ZNF750 and p63 (Supplementary Table 1 and Figure 3e). We further observed a positive correlation between the levels of ZNF750 and p63 transcripts exclusively in squamous-type primary tumours based on TCGA RNA-seq datasets (Figure 3f).

Next, we sought to determine whether ZNF750 controls KLF4 expression in SCC cells. Upregulation of KLF4 transcript level was observed in ZNF750 over-expressing SCC cells (Figure 3g); in contrast, KLF4 mRNA expression decreased in ZNF750 depleted cells (Figure 3h). Notably, the level of KLF4 was positively correlated with ZNF750 expression in SCC cell lines (Figure 3i). Consistently, we found a linear correlation between the mRNA levels of ZNF750 and KLF4 in CSCC, HNSCC and LSCC patient samples from TCGA RNA-seq datasets (Figure 3j). Collectively, these data suggested that ZNF750 is p63-dependent factor and regulates KLF4 expression in SCCs.

Tumour-suppressive property of ZNF750 in SCC cells

To explore the biological relevance of ZNF750 in SCCs, cell line models with ectopic ZNF750 expression were established. Previous studies found that the evolutionarily conserved atypical C2H2 zinc finger motif was required for its transactivation in normal keratinocyte;<sup>5,8</sup> therefore, we performed functional analysis with wildtype as well as C2H2 mutant ZNF750 in a number of

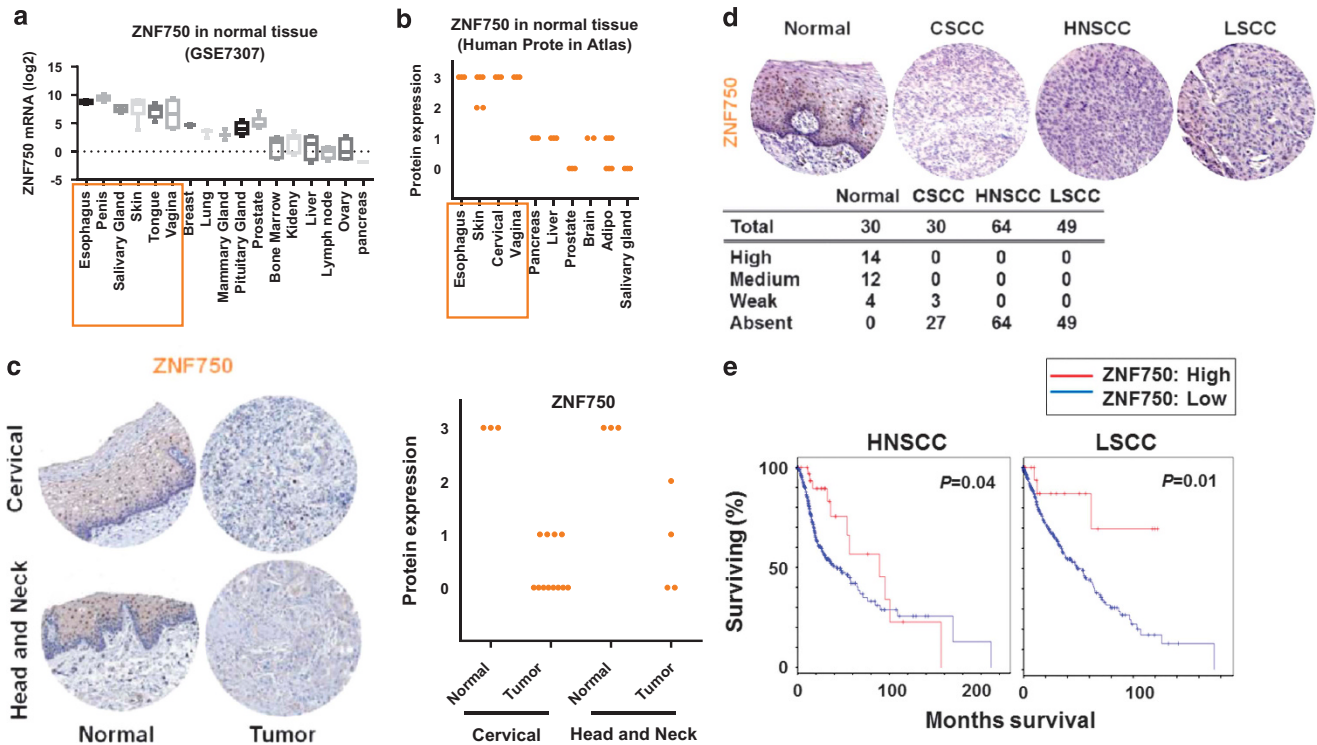


**Figure 2.** ZNF750 is under-expressed in squamous cell carcinomas. **(a)** ZNF750 mRNA expression across normal tissues examined from GEO (series GSE7307). Data show mean  $\pm$  s.d. **(b)** ZNF750 protein expression across normal tissues from Human Protein Atlas (see URL). IHC was performed using anti-ZNF750 antibody (HPA021573, Sigma-Aldrich, St Louis, MO, USA). **(c)** Representative IHC photos (left panel) and IHC scores (right panel) of ZNF750 protein expression in CSCC and HNSCC from Human Protein Atlas. IHC was performed using anti-ZNF750 antibody (HPA023012, Sigma-Aldrich). **(d)** In-house IHC assay of ZNF750 expression in CSCC, HNSCC and LSCC samples. Normal tissues are from cervical tissues ( $\times 10$  magnification). **(e)** Low ZNF750 expression (mRNA expression z-scores (RNA Seq V2 RSEM)  $>$  mean + 1.8 SD or 2.0 SD) was associated with poor disease-free survival of HNSCC and LSCC patients in the TCGA cohorts.

cell lines from either CSCC, skin SCC, HNSCC or LSCC. Exogenous wildtype ZNF750 expression resulted in significant reduction in short-term cell proliferation (Figure 4a and Supplementary Figures 2a and b). In contrast, C2H2 mutant partially or fully lost its inhibitory effect on cell proliferation (Figure 4a). Similarly, wildtype ZNF750, but not C2H2 mutant inhibited foci formation in a variety of SCC cells (Figures 4b and c). The tumour-suppressive potential of ZNF750 was further evaluated by xenograft tumour formation. Importantly, wildtype ZNF750 robustly suppressed tumour growth compared with the control group, whereas the C2H2 mutant had significantly less suppressive ability *in vivo* (Figure 4d). In addition, Ki-67 staining by IHC of xenograft tumours supported our findings that ZNF750 protein decreased the proliferative cell population (Figure 4e). Moreover, the well-defined differentiation marker Involucrin (IVL) was highly expressed in tumours expressing wildtype ZNF750 (Figure 4e). Not surprisingly, neither ZNF750 wildtype nor C2H2 mutant affected p63 expression both *in vivo* and *in vitro* (Supplementary Figures 2c and d). Unaltered p63 transcript level was also observed in ZNF750 depleted cells (Supplementary Figure 2e), in agreement with earlier results<sup>5</sup> showing that ZNF750 was downstream of p63 (Figures 3a and b).

We next addressed whether ZNF750 regulates other important malignant phenotypes. Notably, wildtype ZNF750 potentially inhibited the migration of different types of SCC cells. In sharp contrast, the C2H2 mutant expressing cells showed minimal effect on migration (Figure 4f). We next determined cell adhesion by measuring the efficiency of SCC cells to adhere to collagen type I, and found that this cellular phenotype was significantly impaired by wildtype ZNF750, but was unaffected by the C2H2 mutant

(Figure 4g). As cellular signalling during cell adhesion is associated with anoikis resistance,<sup>9</sup> we examined the effect of ZNF750 on resistance to anoikis of SCC cells (Figures 4h and i). Concomitantly, we attenuated anoikis-resistance only in wildtype ZNF750 but not C2H2 mutant cells. We confirmed that impaired tumour-suppressive functions of the C2H2 mutant was not due to the lack of expression or mis-localization (Supplementary Figures 2f and g). Importantly, ZNF750 hardly affected proliferation in non-SCC cells such as glioblastoma cells (Supplementary Figures 2h and i). Taken together, these data strongly suggest that ZNF750 is a bona fide lineage-specific tumour suppressor, and the C2H2 domain is important for its biological functions in SCCs.

Transcriptome analysis of ZNF750-regulated genes and processes To explore how ZNF750 suppressed SCC cell malignancy, we performed both cDNA microarray and whole transcriptome sequencing (RNA-seq) to measure global alterations in mRNA levels upon ZNF750 restoration. Gene ontology (GO) analysis revealed that ZNF750 activated a subset of genes highly enriched in processes regulating terminal epidermal differentiation similar to the function of ZNF750 in normal keratinocytes (Figure 5a). Notably, genes repressed by ZNF750 were significantly enriched in processes highly relevant to cancer biology, including cell migration, proliferation, adhesion and cell death, all of which were shown to be regulated by ZNF750 in our experiments (Figure 4). Gene set enrichment analysis (GSEA) further confirmed that ZNF750-upregulated genes were associated with an 'epidermal late differentiation signature'<sup>7</sup> (Figure 5b) while ZNF750-



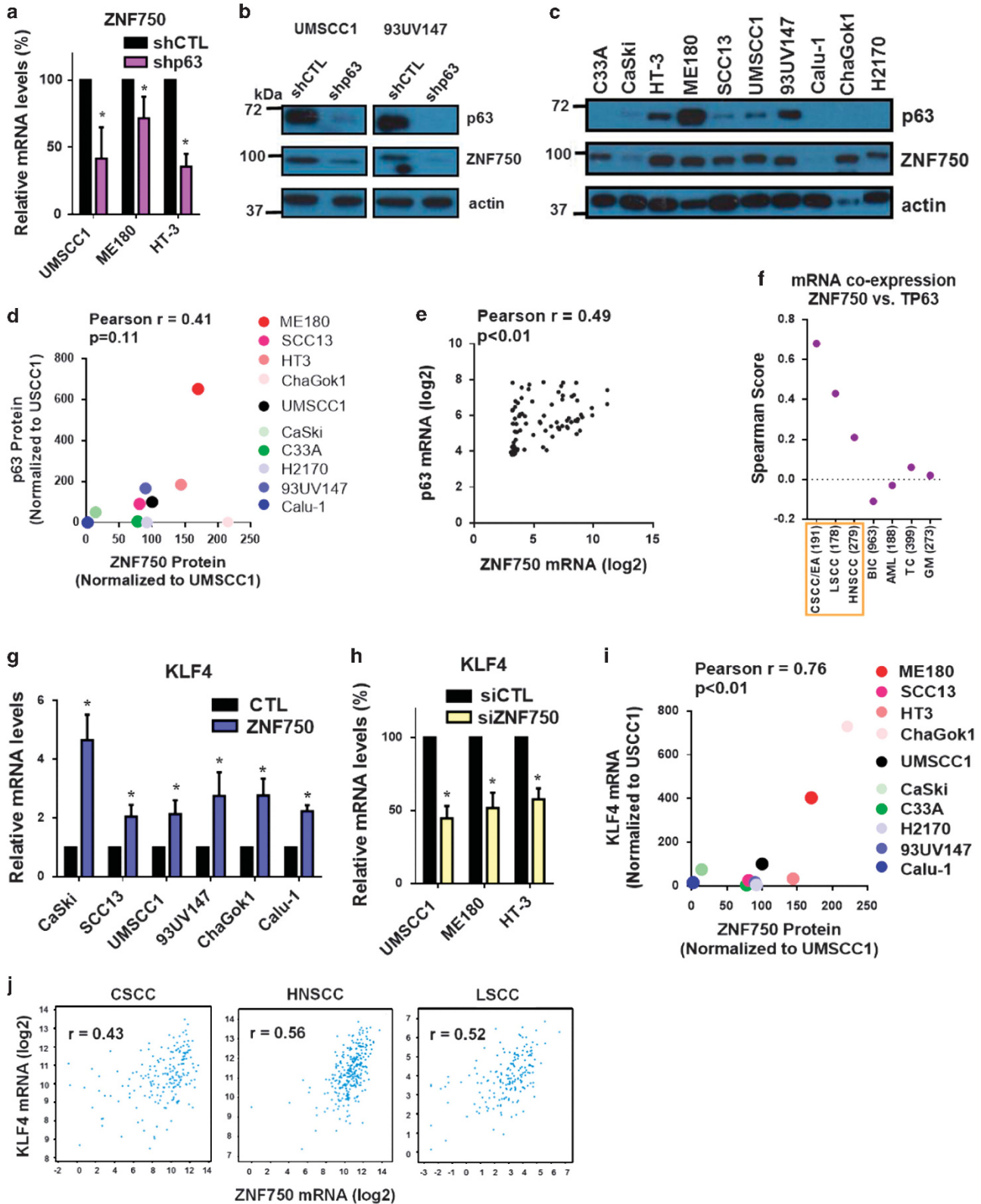


**Figure 3.** ZNF750 is a p63-dependent transcription factor and controls KLF4 expression in SCCs. (a) qRT-PCR analysis of ZNF750 mRNA in SCC cells following p63 depletion. Data show mean  $\pm$  s.d.  $N = 3$ .  $*P < 0.05$ . (b) Western blot analysis of ZNF750 levels in p63-silenced SCC cells. (c, d) Western blot analysis (c) and co-expression analysis (d) of p63 and ZNF750 protein (40  $\mu$ g/lane) levels in various SCC cell lines. (e) Co-expression analysis of ZNF750 mRNA and p63 mRNA in 86 squamous-type cell lines from CCLE (see URL). (f) Summary of correlation coefficients between ZNF750 mRNA and p63 mRNA across different tumour types from TCGA datasets. (g, h) qRT-PCR analysis of KLF4 mRNA in ZNF750 overexpressed SCC cells (g) and ZNF750 depleted SCC cells (h). Data show mean  $\pm$  s.d.  $N = 3$ .  $*P < 0.05$ . (i) Co-expression analysis of KLF4 mRNA and ZNF750 protein (40  $\mu$ g/lane) levels in various SCC cell lines. (j) Co-expression analysis of ZNF750 and KLF4 mRNA based on TCGA dataset.  $r$ ; spearman score.

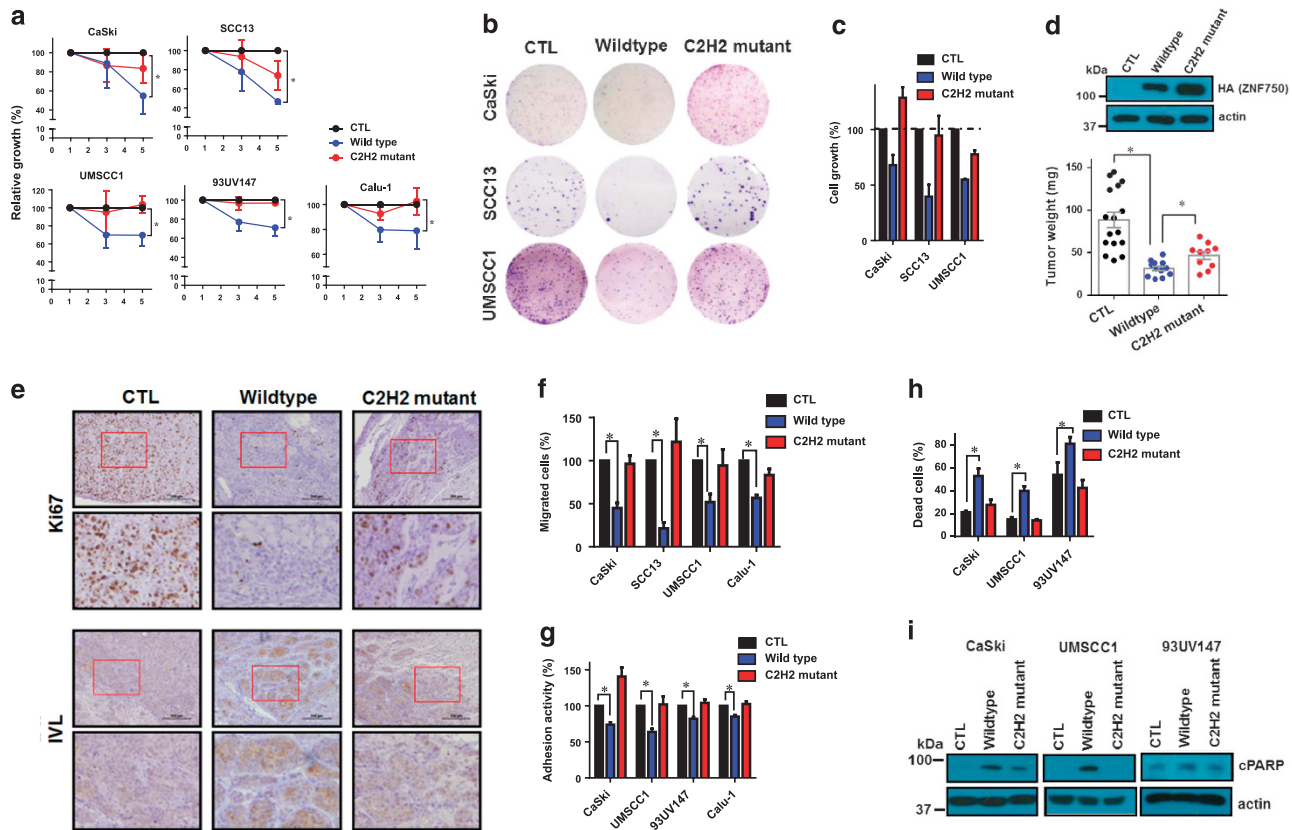


**Figure 4.** Tumour-suppressive properties of ZNF750 in SCCs. (a–c) Short-term proliferation assay (MTT) (a), foci formation assay (b) and the quantification of SCC cell growth (c) either with ectopic expression of GFP control (CTL), wildtype or C2H2 mutant ZNF750. Data show mean  $\pm$  s.d.  $N=3$ .  $*P < 0.05$ . (d) UMSSC1 cells expressing indicated vectors (upper panel) were injected subcutaneously on the upper flanks of NOD-SCID mice, and tumour weights were measured. Data represent mean  $\pm$  s.d.  $*P < 0.05$ . (e) Representative samples of Ki67 and IVL expression detected by IHC in dissected xenograft tumours. (f–g) SCC cells expressing indicated vectors were subjected to migration assay (f) and adhesion assay (g). Data show mean  $\pm$  s.d.  $N=3$  (f) and 4 (g).  $*P < 0.05$ . (h–i), Dead cells (trypan-blue positive) (h) and cleaved-PARP (i) in SCC cells expressing indicated vectors upon anoikis challenge. Data show mean  $\pm$  s.d.  $N=4$  (h).  $*P < 0.05$ .

repressed genes were enriched in an ‘epidermal progenitor signature’<sup>7</sup> (Figure 5b).

LncRNAs have been shown to participate in the regulation of epidermal cell differentiation. To determine whether ZNF750 could regulate the expression of epidermis differentiation-related LncRNAs, we cross-compared LncRNAs whose levels were changed upon ZNF750 activation to those with differential expression during epidermal differentiation<sup>6</sup> (Figure 5c). Interestingly, we identified TINCR as a candidate ZNF750-promoted LncRNA.

Many epidermal progenitor genes contribute to the malignant phenotype of cancer cells, such as uncontrolled proliferation, enhanced migration, EMT and so on.<sup>10</sup> Thus, we hypothesized that ZNF750-mediated repression of epidermal progenitor genes might account for its tumour-suppressive functions in SCC cells, which we observed (Figure 4). We performed similar cross-comparisons, and nominated a total of seven genes as possible ZNF750-repressed progenitor factors, namely THBS1, CTNNAL1, FST, LAMC2, NT5E, NRG1 and COL12A1 (Figure 5d).

#### ZNF750 drives epidermal differentiation in SCCs

Our transcriptome analysis showed that epidermal differentiation was the most significantly enriched process activated by ZNF750 in SCC cells. Therefore, the role of ZNF750 in differentiation regulation in SCCs was further characterized. We first validated

that wildtype ZNF750 induced the epidermal differentiation complex<sup>11</sup> including the small proline-rich proteins 1B (SPRR1B), the calcium-binding protein S100A8 and IVL (Figure 6a and Supplementary Figure 3a), while suppressing the expression of the basal cell marker K14 in a variety of SCC cells (Figure 6b). Confirmation of the pro-differentiation function of ZNF750 was its ability to enhance the level of IVL protein both under organotypic and 2D culture conditions (Figure 6c, and Supplementary Figures 3b and c). Importantly, these changes were only triggered by wildtype but not C2H2 mutant ZNF750 (Figures 6a–c). Concordantly, ablation of endogenous ZNF750 either by siRNA-mediated knockdown or CRISPR/Cas9-mediated genomic disruption decreased the expression of these differentiation factors (Figures 6d and e, and Supplementary Figures 3d and e). Furthermore, interrogation of TCGA RNA-seq datasets showed a linear correlation between the mRNA levels of ZNF750 and epidermal differentiation-related genes in CSCC, HNSCC and LSCC patient samples (Figure 6f). These positive correlations were exclusively observed in squamous-type tumours in TCGA RNA-seq datasets (Figure 6g), again underscoring the lineage-specific role of ZNF750 in cancer biology. We next asked whether differentiation stimuli lead to changes of the level of ZNF750. Consistently, stimuli of keratinocyte differentiation, including high confluence condition<sup>12</sup> or  $Ca^{2+}$  concentration,<sup>8</sup> caused marked induction of ZNF750 expression (Figure 6h and Supplementary Figure 3f). Collectively, these results suggest that ZNF750 strongly promotes

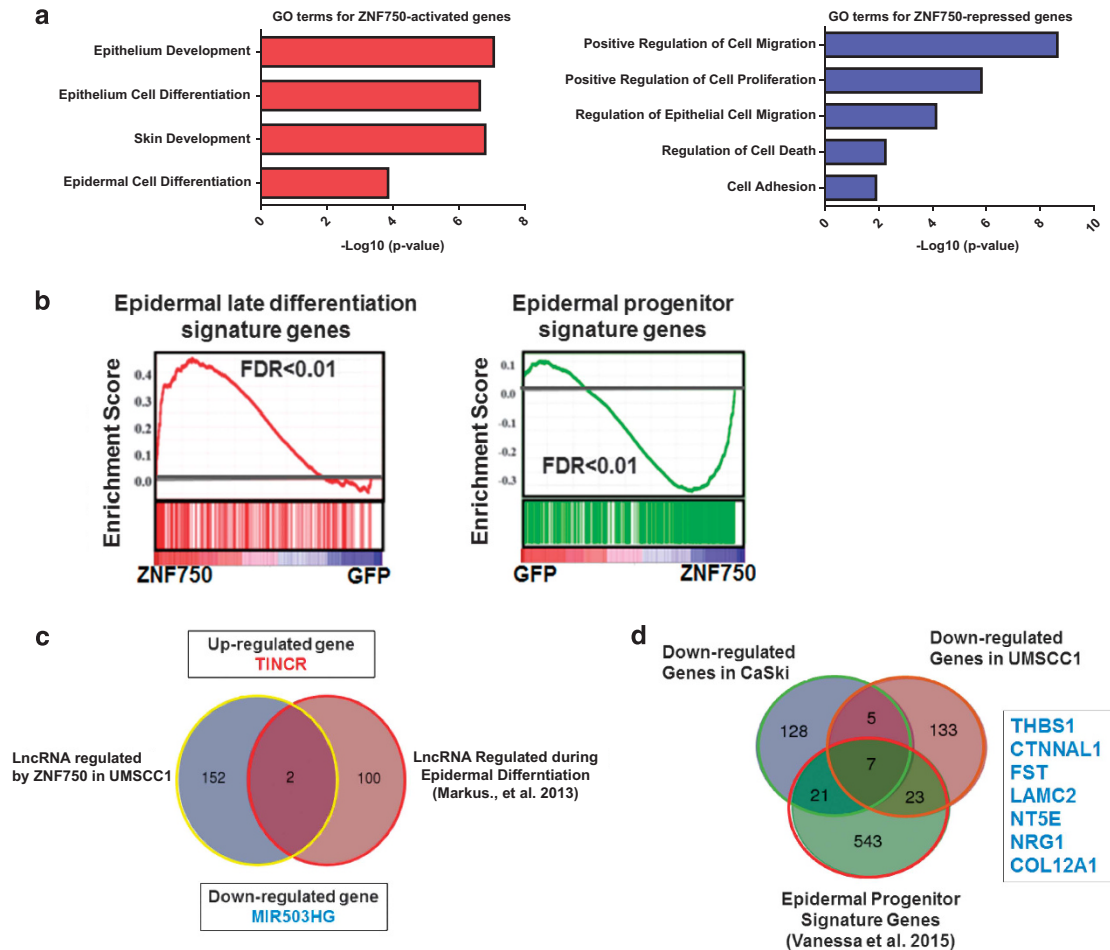


**Figure 5.** Transcriptome analysis of ZNF750-regulated genes and processes. **(a)** GO analysis of ZNF750-activated and -repressed genes measured by RNA-seq comparing cells over-expressing GFP versus ZNF750 protein. **(b)** GSEA of ZNF750-induced genes versus indicated gene signatures. **(c)** Venn diagram illustrating the overlap between LncRNAs regulated by ZNF750 in UMSSC1, and the ones with differential expression patterns during epidermal differentiation reported by Kretz *et al.*<sup>6</sup> **(d)** Venn diagram illustrating the overlap between ZNF750-dependent repressed genes and epidermal progenitor signature genes reported by Vanessa *et al.*<sup>7</sup>

epidermal differentiation through induction of a number of differentiation-related factors in various types of SCC cells.

To determine further whether ZNF750 regulates the differentiation of non-malignant cells, such as keratinocytes, the expression levels of epidermal differentiation factors were measured in HaCaT (non-malignant keratinocytes<sup>13</sup>) by qRT-PCR after siRNA-mediated ZNF750 depletion (Figure 6i). Indeed, differentiation genes were suppressed in ZNF750 silenced HaCaT cells (Figure 6i), highlighting the role of ZNF750 in enabling epidermal differentiation.

ZNF750 regulation of TINCR LncRNA mediates differentiation, cell growth and cell migration in SCCs

TINCR was identified as a ZNF750-regulated LncRNA; however, its roles in the settings of SCC are unknown. We next sought to understand whether and how TINCR is involved in the biology of SCCs and its relationship with ZNF750. In order to define the regulation between TINCR and ZNF750, we first confirmed the upregulation of TINCR transcripts in ZNF750 over-expressing SCC cells (Figure 7a), and the downregulation of TINCR in ZNF750 depleted cells (Figure 7b). Of note, TINCR transcript levels were significantly correlated with ZNF750 protein levels in SCC cell lines (Figure 7c). Moreover, transcripts of both TINCR and ZNF750 are

activated during epidermal lineage induction (unpublished data) (Figure 7d). Furthermore, we observed a positive correlation between the levels of ZNF750 and TINCR transcripts exclusively in squamous-type tumours on TCGA RNA-seq datasets (Figures 7e and f), suggesting that ZNF750 can activate both LncRNAs (such as TINCR) and coding genes in SCCs.

Next, to explore the role of TINCR in SCC biology, we asked whether TINCR regulates SCC cell malignancy. Depletion of TINCR by siRNA resulted in an increased cell growth as well as migration activity (Supplementary Figures 4a–c). Moreover, silencing of TINCR resulted in the decrease of differentiation-related gene (Supplementary Figure 4d). We next probed whether TINCR was involved in ZNF750-mediated functions. Importantly, TINCR depletion partially rescued ZNF750-repressed malignancies, including cell growth (Figures 7g and h) and migration (Figure 7i). Silencing of TINCR also impaired the activation of differentiation-related gene by ZNF750 (Figure 7j). In addition, Kaplan–Meier analysis revealed that low levels of TINCR were significantly correlated with poor outcome of patients with HNSCC (Log-rank test,  $P=0.03$ ) in the TCGA cohort (Figure 7k). Collectively, these results strongly suggest that as one of the downstream targets of ZNF750, TINCR mediates the tumour-suppressive function of ZNF750 in SCC cells.



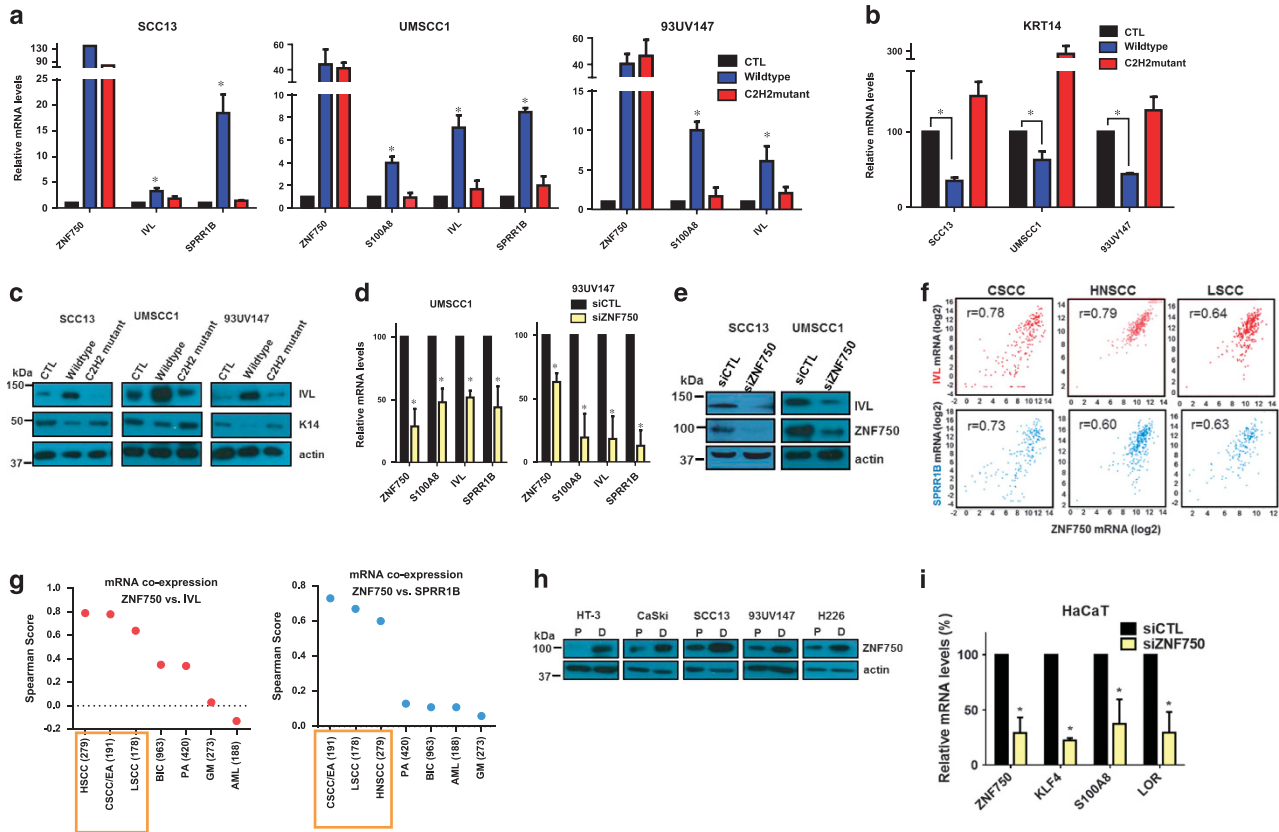


**Figure 6.** ZNF750 regulates epidermal differentiation in a variety of SCC cells. **(a)** qRT-PCR analysis of differentiation related genes and **(b)** basal cell marker K14 gene in SCC cells expressing indicated vectors. Data show mean  $\pm$  s.d.  $N = 3$ .  $*P < 0.05$ . **(c)** Western blot analysis of IVL and K14 levels in SCC cells expressing indicated vectors. **(d)** qRT-PCR analysis of differentiation related genes in SCC cells treated with either scrambled siRNAs (siCTL) or ZNF750 siRNAs (siZNF750). Data show mean  $\pm$  s.d.  $N = 3$ .  $*P < 0.05$ . **(e)** Western blot analysis of IVL and K14 levels in SCC cells treated with indicated siRNA. **(f)** Co-expression analysis of ZNF750 mRNA and epidermal differentiation gene mRNA based on TCGA dataset.  $r$ ; spearman score. **(g)** Summary of correlation coefficient between the mRNA levels of ZNF750 and indicated differentiation genes across different tumour types from TCGA. **(h)** Western blot analysis of ZNF750 protein levels in SCC cells under proliferative condition (cells  $< 50\%$  confluent) (P) or differentiation condition (super confluent) (D) *in vitro*. **(i)** qRT-PCR analysis of differentiation related genes including KLF4 in non-SCC cell line HaCaT treated with scrambled siRNAs (siCTL) or ZNF750 siRNAs (siZNF750). Data show mean  $\pm$  s.d.  $N = 3$ .  $*P < 0.05$ .

**Transcriptional repression of LAMC2 by ZNF750 in SCC cells**

LAMC2 is one of the seven candidate progenitor genes repressed by ZNF750 (Figure 5d). We and others previously have shown that LAMC2 promoted the proliferation and migration of several types of cancer cells.<sup>14–19</sup> Thus, we hypothesized that transcriptional repression of LAMC2 by ZNF750 might partially account for its tumour-suppressive activities. To determine whether ZNF750 regulates LAMC2 at the transcriptional level, we measured the levels of LAMC2 transcript and protein upon forced expression of either wildtype or C2H2 mutant ZNF750 (Figures 8a and b). LAMC2 expression was robustly decreased by wildtype but not C2H2 mutant ZNF750. A recent study found that ZNF750 interacted with target genes through recognizing the ‘CCNAGGC’ DNA motif.<sup>8</sup> Thus, we searched for this motif near the transcription starting site of LAMC2, and identified it within regions of R2, R3, R4 (Figure 8c). R1 region that does not contain the motif was prepared as a negative control. ChIP-PCR results showed a prominent binding of ZNF750 to the R2 region (Figure 8d). To examine if this DNA region is responsible for ZNF750-mediated transcriptional regulation of LAMC2, dual-reporter luciferase assay was performed (Figure 8e). Importantly, wildtype ZNF750 strongly suppressed the luciferase activity of R2 in 293 T cells (Figure 8e). These data indicate that ZNF750 directly inhibits the transcription of LAMC2 in SCC cells.

We next asked whether LAMC2 was involved in ZNF750-regulated cell migration. Depletion of LAMC2 inhibited cell migration (Supplementary Figures 5a and b), whereas over-expression of LAMC2 enhanced this process (Supplementary Figures 5c and d). Rescue experiments showed that re-introduction of LAMC2 in cells over-expressing ZNF750 significantly elevated the impaired cells’ migration (Figures 8f and g). Taken together, these results strongly suggest that ZNF750 suppresses SCC cell migration by directly inhibiting LAMC2 transcription.

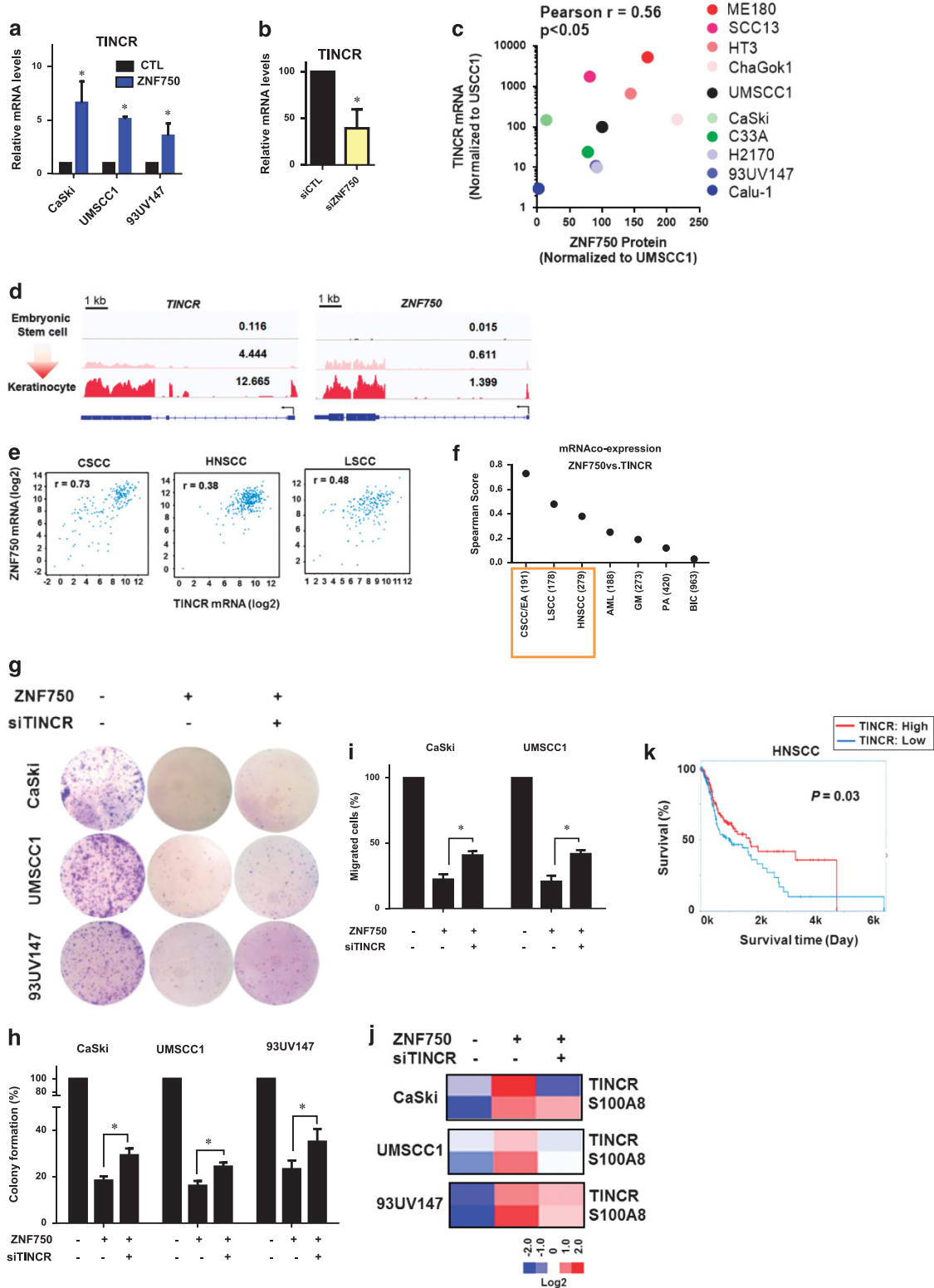
**DISCUSSION**

In this study, we demonstrated genomic and expression abnormalities and biological relevance of ZNF750, which is exclusive in human SCCs. Interestingly, TINCR lncRNA participated in control of cellular proliferation, migration and differentiation downstream of ZNF750. Furthermore, ZNF750 suppressed migration of SCC cells by directly inhibiting transactivation of LAMC2.

Genome instability is one of the hallmarks of cancer, and somatic mutation and copy number loss are major causes of the inactivation of tumour suppressors. Based on our genomic analysis in three major types of human SCCs (CSCC, HNSCC and LSCC), 4.5% of ZNF750 mutations lead to detrimental frameshifts or premature truncations of ZNF750 protein. In addition, many

mutations were identified within the first 100 amino acids, which encodes for the evolutionally conserved C2H2 DNA-binding domain. We functionally validated that mutation of this domain resulted in its loss of function. A recent report studying normal keratinocytes also demonstrated that mutation of the C2H2

destroyed the ability of ZNF750 to activate differentiation genes.<sup>5,8</sup> Moreover, a cancer-derived mutant, ZNF750 S70X, caused mislocalization and abrogated its tumour suppressing function in ESCC.<sup>4</sup> Collectively, these data suggest that somatic mutations compromise ZNF750 function during tumorigenesis.





We further confirmed the downregulation of ZNF750 expression in these SCCs, which is consistent with its expression profiles in ESCC.<sup>3,4</sup> We also report, for the first time, the prognostic value of ZNF750 expression in all major SCCs, highlighting the biological relevance of ZNF750 in these malignancies.

Tumour differentiation is an important clinical-pathological parameter affecting malignant potential.<sup>10,20</sup> Here, we showed that restoration of ZNF750 in SCCs cells activated a number of epidermal differentiation genes such as IVL, SPRR1B and S100A8. Importantly, these differentiation-related genes have been shown to be functionally relevant in SCCs. For example, S100A8/S100A9 were recently reported to inhibit G2/M progression and cell growth through enhancing PP2A phosphatase activity in HNSCC cells.<sup>21</sup> In addition, S100A8/S100A14 inhibited the oncogenic function of HPV16 E7 protein through regulating Casein Kinase II-dependent phosphorylation of E7.<sup>22</sup> Thus, ZNF750-regulated differentiation genes not only serve as markers of cellular differentiation but also modulate SCC cellular functions.

We found that TINCR lncRNA mediates biological functions downstream of ZNF750. Recently, Kretz *et al* reported decreased TINCR expression in human SCC samples,<sup>6</sup> implying that TINCR has a tumour-suppressive role. However, oncogenic functions of TINCR through inhibiting KLF2 in gastric cancer was also observed recently.<sup>23</sup> Endogenous levels of KLF2 are undetectable in SCCs (unpublished data); therefore, the cancer-related function of TINCR might be context-dependent requiring further investigation.

In summary, we show that somatic inactivation and decrease expression of ZNF750 contributes to the pathogenesis of SCC, and that ZNF750 expression is a novel biomarker for SCC prognosis. Through a variety of detailed mechanistic studies, both TINCR and LAMC2 were identified as functional downstream factors of ZNF750. These data will shed light on the understanding of the molecular basis of SCC biology.

## MATERIALS AND METHODS

### Cell culture

HEK293T (kindly provided by Dr Yoshiaki Ito, Cancer Science Institute of Singapore), CSCC cell lines (C33A, CaSki, HT-3, ME180 and SiHa), skin SCC (SCC13), HNSCC cell lines (UMSCC1 and 93UV147) (kindly provided by Dr Timothy Chan, Memorial Sloan Kettering Cancer Center), and a spontaneously immortalized human keratinocyte cell line (HaCaT, kindly provided by Dr Norbert Fusenig, German Cancer Research Centre) were maintained in Dulbecco's Modified Eagle Medium supplemented with 10% (vol/vol) fetal bovine serum and 1% (vol/vol) penicillin/streptomycin (P/S), and LSCC cell lines (Calu-1, ChagoK1, H2170 and H226, kindly provided by Dr GOH Boon Cher, Cancer Science Institute of Singapore) were maintained in RPMI1640 supplemented with 10% fetal bovine serum and 1% P/S, at 37 °C, 5% CO<sub>2</sub> in a humidified atmosphere. Cell lines were recently tested for the absence of mycoplasma. Cell lines were authenticated by short tandem repeat analysis with the Geneprint 10 System Kit (B9510, Promega, Madison, WI, USA) in 2014.

### Cell proliferation assay

SCC cells were seeded into a 96-well plate at 3000 cells/well and cultured for the indicated time courses. Cell viability was assessed using the MTT (3-(4, 5-dimethylthiazol-2-yl)-2, 5-diphenyltetrazolium bromide) method. In brief, 10 µL of 12 mM MTT solution was added into each well followed by 3 h incubation, which was stopped by adding 100 µL of STOP solution (2% acetic acid, 16% SDS, 42% DMF). Samples were mixed thoroughly and measured at 570 nm for absorbance.

### Foci formation assay

SCC cells were seeded into six-well plates at 1000 cells/well and cultured for 10 days, followed by fixation, staining with crystal violet and photographing the cells. For quantification, staining was dissolved in MTT stop solution, and measured at 570 nm for absorbance.

### Migration assay

SCC cells were seeded onto transwell inserts (3422, Corning, Kennebunk, ME, USA) in 24-well plates and incubated for 48 h. The inserts were washed with PBS, and non-migrating cells were wiped off the top side. Migrated cells were fixed with 4% paraformaldehyde, stained with 4',6-diamidino-2-phenylindole (DAPI), and nuclei were counted.

### Adhesion assay

Ninety-six-well tissue culture plates were coated with COL-I at 37 °C for 1 h and rinsed with PBS. SCC cells were added to each well, and cells were allowed to incubate at 37 °C for 30 min. After washing, adherent cells were estimated by MTT method described earlier.

### Western blotting

Cells were lysed with lysis buffer (20 mM HEPES (pH 7.4), 350 mM sodium chloride, 1.5 mM magnesium chloride, 1 mM EGTA, 10% (v/v) glycerol, 1% Triton X-100, a mixture of protease inhibitors (Roche, Indianapolis, IN, USA), 0.2 mmol/L sodium orthovanadate and 1 mmol/L phenylmethylsulfonyl fluoride). BCA assay (Santa Cruz, Dallas, TX, USA) was used for protein quantification. Cell lysates or immunoprecipitation elutes were subjected to SDS-PAGE followed by conventional wet transfer. Membranes were incubated with antibodies as indicated and exposed to secondary horseradish peroxidase-conjugated antibodies (Millipore, Billerica, MA, USA). Antibodies used in this study were listed in Supplementary Table S2. The relative amount of p63 and ZNF750 protein was quantified by densitometry using Photoshop CS6 Extended (Adobe, San Jose, CA, USA) and normalized by GAPDH. Values from each cell line were then divided by that of UMSCC1.

### Tissue micro array and IHC

Human cervix cancer tissue array (OD-CT-RpUtr03-006, 30 normal cervical tissues and 30 CSCC tissues), head and neck tissue array (HN803c, 64 HNSCC tissues), and lung SCC tissue array (LC1505, 49 LSCC tissues) were obtained from US Biomax Inc. (Rockville, MD, USA). In the IHC experiment, the slides were deparaffinized and blocked with goat serum for 30 min at room temperature, followed by incubation with rabbit anti-ZNF750 (1:50; HPA023012, Sigma-Aldrich, St Louis, MO, USA) overnight at 4 °C. After incubation with horseradish peroxidase-linked secondary antibody (Dako, Tokyo, Japan) for 60 min, slides were counterstained with Mayer's hematoxylin. The degree of immunostaining was viewed and scored

**Figure 7.** LncRNA TINCR mediates the function of ZNF750. **(a)** qRT-PCR analysis of TINCR in SCC cells either with ectopic expression of GFP control (CTL) or wildtype ZNF750 and **(b)** in ME180 cells (CSCC) transfected with either scrambled siRNAs (siCTL) or ZNF750 siRNAs (siZNF750). Data show mean ± s.d. *N* = 3–6. \**P* < 0.05. **(c)** Co-expression analysis of TINCR transcripts and ZNF750 protein (40 µg/lane) levels in variety of SCC cell lines. **(d)** Human H1 embryonic stem cells were differentiated to keratinocyte progenitors *in vitro*, and the global RNA expression profile during differentiation were analysed using RNA-seq. Sequencing reads after normalization spanning ZNF750 gene are shown. Numbers indicate FPKM value (Fragments Per Kilobase of Exon per Million Fragments Mapped). **(e)** Co-expression analysis of ZNF750 mRNA and TINCR transcripts from TCGA dataset. **(f)** Summary of correlation coefficient between ZNF750 mRNA and TINCR transcripts across different tumour types from TCGA dataset. **(g)** SCC cells expressing either GFP (CTL, control) or wildtype ZNF750 were transfected with either scrambled or TINCR siRNAs and then subjected to foci formation assay (representative photos), and **(h)** foci were quantified. Data show mean ± s.d. *N* = 4. \**P* < 0.05. **(i)** SCC cells with indicated treatment were subjected to migration assay. **(j)** Effects of TINCR knockdown on differentiation-related gene expression; heatmaps show average fold change measured by qRT-PCR (*N* = 3). **(k)** Low TINCR expression is associated with poor disease-free survival of HNSCC patients on TCGA cohort.

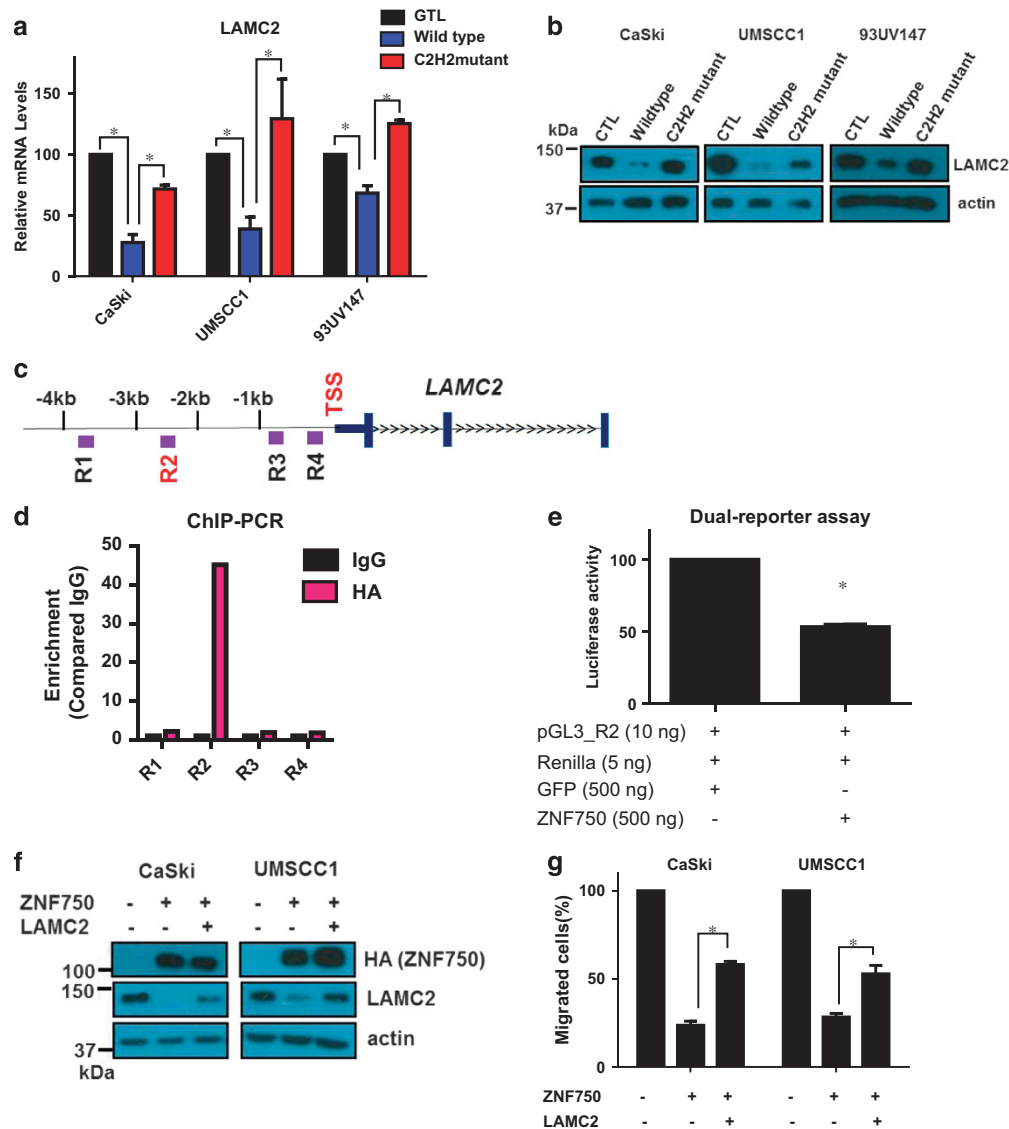


**Figure 8.** ZNF750 represses LAMC2 transactivation. (a) qRT-PCR analysis of LAMC2 mRNA levels in SCC cells expressing indicated vectors. Data show mean  $\pm$  s.d.  $N=3$ . \* $P < 0.05$ . (b) Western blot analysis of LAMC2 levels in SCC cells expressing indicated vectors. (c) ZNF750 motifs present in R2, R3 and R4 DNA fragments 5' upstream of LAMC2 (R1: nucleotide (nt) - 3701/- 3528; R2: nt - 2506/- 2273; R3: nt - 737/- 570; R4: nt - 346/- 182) (lower). (d) ChIP-PCR analysis of DNA fragments pulled down by an anti-HA antibody. IgG was used as a negative control. Representative data are shown.  $N=3$ . (e) 293 T cells transfected with the reporter constructs pGL3-(R2), renilla, and either GFP or wildtype ZNF750. Renilla and luciferase activity was analysed. Data show mean  $\pm$  s.d.  $N=3$ . \* $P < 0.05$ . (f) Western blot analysis of LAMC2 and ZNF750 levels in SCC cells in indicated conditions. (g) SCC cells in indicated conditions were subjected to migration assay. Data show mean  $\pm$  s.d.  $N=3$ . \* $P < 0.05$ .

separately by two independent investigators without any prior knowledge of clinicopathologic data. Expression of ZNF750 was scored as either absent, weak (faint staining in  $< 25\%$  of tumour cells), medium (moderate staining in  $25- < 75\%$ ) or high (moderate staining in  $75\%$ ).

#### cDNA vectors, shRNA vectors and siRNAs

Expression vectors pLEX-ZNF750 (wildtype) and pLEX-C2H2 mutant ZNF750 (C2H2 mutant) were generously provided by Dr Paul A. Khavari (Stanford University School of Medicine). We also used another ZNF750 expression vector, SHC003-ZNF750 (which we reported previously<sup>3</sup>), in some of the experiments to confirm that the results were not affected by different vector systems (Supplementary Figure 6). The shRNA construct for p63 was made with PLKO.1 backbone (Sigma-Aldrich) using Age I and EcoR I sites (Supplementary Table S3). LAMC2 over-expression and shRNA vectors were described previously.<sup>24</sup> Pooled siRNAs targeting human ZNF750 (M-014417-01) and TINCR (R-015725-00-0005) and scramble siRNA

(D-001210-01) were purchased from Thermo Scientific (Rockford, IL, USA) (Supplementary Table S3).

#### Transfections, viral particle production and infection

DNA and siRNA transfections were performed using Lipofectamine 2000 and Lipofectamine RNAiMAX (Life Technologies, Carlsbad, CA, USA), respectively. Lentiviral particles were produced with the MISSION Lentiviral Packaging System (Sigma-Aldrich). SCCs cells were transduced with the lentiviral particles in the presence of 8  $\mu\text{g/ml}$  polybrene (Sigma-Aldrich) for 48 h.

#### cDNA preparation and quantitative real-time RT-PCR assay

Quantitative real time RT-PCR was performed by KAPA SYBR qPCR kits (KAPA Biosystems, Wilmington, MA, USA) in a 7500 real-time PCR system (Applied Biosystems, Foster City, CA, USA) according to the manufacturer's instructions. The relative mRNA expression level of target genes was

calculated using GAPDH as a loading control. The primers are listed in Supplementary Table S4.

### Xenograft growth assay

Female, 5–6 weeks, non-obese diabetic severe combined immunodeficient (NOD-SCID) mice were randomly allocated to control and experimental cohorts. Eight mice were used for control cohort; six and five mice were used for wildtype and C2H2 mutant groups, respectively. Three million UMSSC1 cells transduced with GFP (Control), wildtype or C2H2 mutant were mixed with 100  $\mu$ l of Matrigel (BD Biosciences, San Jose, CA, USA) and injected subcutaneously in the upper flanks of the NOD-SCID mice. After 5 weeks, mice were euthanized; tumours were dissected and weighted. No blinding of investigators was performed. No statistical methods were used to determine the sample size of mice. The experiment was performed in compliance with ethical regulations of the Institutional Animal Care and Use Committee of the National University of Singapore.

### Chromatin Immuno-precipitation (ChIP) assay

Formaldehyde was used to cross-link proteins to DNA. Cells were lysed with buffer A (10 mM HEPES, pH 7.9, 10 mM KCl, 0.1 mM EDTA, 0.1 mM EGTA, 0.5% NP-40). Nuclei were pelleted at 12 000 rpm for 5 min and lysed in 800  $\mu$ l lysis buffer (50 mM Tris-HCl, pH 8.0, 10 mM EDTA, 1% SDS). Cell lysates were sonicated using a Bioruptor ultrasonic cell disruptor to shear genomic DNA to an average fragment size of 150–250 bp, and immunoprecipitation was performed using Chip-grade HA antibody (ab9110, Abcam, Cambridge, MA, USA). One microgram of primary antibody/10 million cells was incubated with precleared chromatin for 16 h. Protein A/G dynabeads were added for 1 h and followed with increasing stringency washes with cold low salt wash buffer, high salt wash buffer, LiCl wash buffer and TE buffer. Bound DNA was eluted by the buffer containing 1% SDS and 0.1 M NaHCO<sub>3</sub>, reverse-crosslinked overnight at 65 °C, purified using a QIAquick PCR purification kit (QIAGEN, Hilden, Germany). The primers used for PCR amplification of the precipitated DNA fragments are R1 forward 5'-GATTACCCATGCTGTGTATGT-3', R1 reverse 5'-CCTTTAATTAACACATGGCTTTTCA-3'; R2 forward 5'-CAAGCTGAGCCA GACAGTT-3', R2 reverse 5'-CCACCAGCAGCCTCTTTTAT-3'; R3 forward 5'-C ACCAAGTCAAGCTAGATACTATT-3'; R3 reverse 5'-GACGAGGTCTTGCTG TGTG-3'; R4 forward 5'-TAACCTGGTGAGCAGGAAG-3', R4 reverse 5'-C TCCGGCTTAAAGGACATCA-3'.

### Reporter assay

Four individual fragments (R2: nucleotide (nt) –2506/–2273 was cloned from UMSSC1 cells into pGL3 vector using multi-cloning sites (XhoI/MluI). Primer pairs for cloning are XhoI-R2 forward 5'-AAAACGCGTGGA GCAAGGTAAGGGAT-3' and MluI-R2 reverse 5'-TTTCTCGAGCGCAAAT GGACACA-3'.

The Dual Luciferase Reporter Assay system (Promega) was used according to the manufacturer's instructions. In brief, 293 T cells were seeded into 24-well plates and co-transfected with pGL3-R2, pRL-TK, plus either GFP or wildtype ZNF750. After 48 h, the levels of renilla and luciferase activity was measured.

### Bioinformatics and data analysis

Copy number data of various SCC types including C5CC, HNSCC and LSCC were collected from TCGA (see URL) via cBio Cancer Genomics Portal (see URL) and analysed by IGV software (see URL). Somatic mutation profiles of ZNF750 in ESCC were obtained from previous reports by Lin *et al* and Zhang *et al*.<sup>3,4</sup> (Figures 1a and b). Mutation and deletion results of ZNF750 across various cancers were from TCGA (Figure 1c). ZNF750 mRNA expression in normal tissues were examined based on GEO (see URL, GSE7307) (Figure 2a). ZNF750 mRNA-expression and survival data in HNSCC and LSCC were obtained from TCGA via cBio Cancer Genomics Portal (Figure 2e). Spearman correlation values were analysed through TCGA via cBio Cancer Genomics Portal (Figures 3f and j, Figures 6f and g, Figures 7e and f). ZNF750 protein expression levels were obtained from Human Protein Atlas (Figures 2b and c). Expression profiles of ZNF750 and p63 in squamous cancer cell lines were determined based on CCLE (see URL) (Figure 3e). TINCR expression and survival data in HNSCC were from TCGA via The Atlas of ncRNA in Cancer (Figure 7k). All datasets were accessed and analysed by 1 July 2015. GO analysis was performed using ConsensusPathDB (see URL). GSEA was performed with GSEA v2.2.2 software (see URL).

### Statistical analyses

The following experiments (cell proliferation assay, anchorage-dependent colony formation assay, migration assay, adhesion assay, anoikis assay, real time RT-PCR analysis and luciferase reporter assay) were performed in triplicate ( $n=3$ ) and independently replicated three or four times. Data were shown as average of biological replicates ( $N=3$  or 4). Two-tailed Student's *t*-test was performed upon verification of the assumptions (for example, normality), otherwise the non-parametric test was applied by GrafPad Prism. We performed correlation analysis and calculated Pearson correlation value using GrafPad Prism.  $P < 0.05$  was considered statistically significant.

### URLs

The Cancer Genome Atlas (TCGA), <http://cancergenome.nih.gov/>; Integrated Genomics Viewer (IGV), <http://www.broadinstitute.org/igv/>; cBio Cancer Genomics Portal, <http://www.cbioportal.org/>; Human Protein Atlas, <http://www.proteinatlas.org/>; Gene Expression Omnibus (GEO), <http://www.ncbi.nlm.nih.gov/geo/>; The Atlas of ncRNA in Cancer (TANRIC), [http://ibl.mdanderson.org/tanric/\\_design/basic/index.html](http://ibl.mdanderson.org/tanric/_design/basic/index.html); Cancer Cell Line Encyclopedia (CCLE), <http://portals.broadinstitute.org/ccle/>; Gene Set Enrichment Analysis (GSEA), <http://software.broadinstitute.org/gsea/>; ConsensusPathDB, <http://consensuspathdb.org/>.

### CONFLICT OF INTEREST

The authors declare no conflict of interest.

### ACKNOWLEDGEMENTS

This work was funded by the Singapore Ministry of Health's National Medical Research Council (NMRC) under its Singapore Translational Research (STaR) Investigator Award to HPK, NMRC Individual Research Grant (NMRC/1311/2011) and the NMRC Centre Grant awarded to National University Cancer Institute of Singapore, the National Research Foundation Singapore and the Singapore Ministry of Education under its Research Centres of Excellence initiatives. D-CL was supported by American Society of Hematology Fellow Scholar Award, Donna and Jesse Garber Awards for Cancer Research, National Center for Advancing Translational Sciences UCLA CTSI Grant UL1TR000124. This study was partially supported by a generous donation from the Melamed family. This research was also supported by the RNA Biology Center at the Cancer Science Institute of Singapore, NUS, as part of funding under the Singapore Ministry of Education's Tier 3 grants, grant number MOE2014-T3-1-006.

### ACCESSION CODE

cDNA micro array and RNA-seq files have been deposited into Gene Expression Omnibus (GSE86015).

### REFERENCES

- 1 American Cancer Society. *Cancer Facts and Figures 2011*. American Cancer Society: Atlanta, 2011.
- 2 Jemal A, Siegel R, Ward E, Hao Y, Xu J, Murray T *et al*. Cancer statistics, 2008. *CA Cancer J Clin* 2008; **58**: 71–96.
- 3 Lin DC, Hao JJ, Nagata Y, Xu L, Shang L, Meng X *et al*. Genomic and molecular characterization of esophageal squamous cell carcinoma. *Nat Genet* 2014; **46**: 467–473.
- 4 Zhang L, Zhou Y, Cheng C, Cui H, Cheng L, Kong P *et al*. Genomic analyses reveal mutational signatures and frequently altered genes in esophageal squamous cell carcinoma. *Am J Hum Genet* 2015; **4**: 597–611.
- 5 Sen GL, Boxer LD, Webster DE, Bussat RT, Qu K, Zarnegar BJ *et al*. ZNF750 is a p63 target gene that induces KLF4 to drive terminal epidermal differentiation. *Dev Cell* 2012; **22**: 669–677.
- 6 Kretz M, Siprashvili Z, Chu C, Webster DE, Zehnder A, Qu K *et al*. Control of somatic tissue differentiation by the long non-coding RNA TINCR. *Nature* 2013; **493**: 231–235.
- 7 Lopez-Pajares V, Qu K, Zhang J, Webster DE, Barajas BC, Siprashvili Z *et al*. A LncRNA-MAF:MAFB transcription factor network regulates epidermal differentiation. *Dev Cell* 2015; **6**: 693–706.
- 8 Boxer LD, Barajas B, Tao S, Zhang J, Khavari PA. ZNF750 interacts with KLF4 and RCOR1, KDM1A, and CTBP1/2 chromatin regulators to repress epidermal progenitor genes and induce differentiation genes. *Genes Dev* 2014; **18**: 2013–2026.

- 9 Zhong X, Rescorla FJ. Cell surface adhesion molecules and adhesion-initiated signaling: understanding of anoikis resistance mechanisms and therapeutic opportunities. *Cell Signal* 2012; **24**: 393–401.
- 10 Rothenberg SM, Ellisen LW. The molecular pathogenesis of head and neck squamous cell carcinoma. *J Clin Invest* 2012; **6**: 1951–1957.
- 11 Kypriotou M, Huber M, Hohl D. The human epidermal differentiation complex: cornified envelope precursors, S100 proteins and the 'fused genes' family. *Exp Dermatol* 2012; **9**: 643–649.
- 12 Brooks YS, Ostano P, Jo SH, Dai J, Getsios S, Dziunycz P *et al*. Multifactorial ER $\beta$  and NOTCH1 control of squamous differentiation and cancer. *J Clin Invest* 2014; **5**: 2260–2276.
- 13 Boukamp P, Petrussevska RT, Breitkreutz D, Hornung J, Markham A, Fusenig NE. Normal keratinization in a spontaneously immortalized aneuploid human keratinocyte cell line. *J Cell Biol*. 1988; **106**: 761–771.
- 14 Ono Y, Nakanishi Y, Ino Y, Niki T, Yamada T, Yoshimura K, Saikawa M *et al*. Clinicopathologic significance of laminin 5 gamma2 chain expression in squamous cell carcinoma of the tongue: immunohistochemical analysis of 67 lesions. *Cancer* 1999; **85**: 2315–2321.
- 15 Yamamoto H, Itoh F, Iku S, Hosokawa M, Imai K. Expression of the gamma(2) chain of laminin-5 at the invasive front is associated with recurrence and poor prognosis in human esophageal squamous cell carcinoma. *Clin Cancer Res* 2001; **4**: 896–900.
- 16 Hlubek F, Jung A, Kotzor N, Kirchner T, Brabletz T. Expression of the invasion factor laminin gamma2 in colorectal carcinomas is regulated by beta-catenin. *Cancer Res* 2001; **22**: 8089–8093.
- 17 Degen M, Natarajan E, Barron P, Widlund HR, Rheinwald JG. MAPK/ERK-dependent translation factor hyperactivation and dysregulated laminin  $\gamma$ 2 expression in oral dysplasia and squamous cell carcinoma. *Am J Pathol* 2012; **6**: 2462–2478.
- 18 Hamasaki H, Koga K, Aoki M, Hamasaki M, Koshikawa N, Seiki M *et al*. Expression of laminin 5- $\gamma$ 2 chain in cutaneous squamous cell carcinoma and its role in tumor invasion. *Br J Cancer*. 2011; **6**: 824–832.
- 19 Garg M, Braunstein G, Koeffler HP. LAMC2 as a therapeutic target for cancers. *Expert Opin Ther Targets* 2014; **9**: 979–982.
- 20 Ohashi S, Miyamoto S, Kikuchi O, Goto T, Amanuma Y, Muto M. Recent advances from basic and clinical studies of esophageal squamous cell carcinoma. *Gastroenterology* 2015; **149**: 1700–1715.
- 21 Khammanivong A, Wang C, Sorenson BS, Ross KF, Herzberg MC. S100A8/A9 (calprotectin) negatively regulates G2/M cell cycle progression and growth of squamous cell carcinoma. *PLoS One* 2013; **8**: e69395.
- 22 Tugizov S, Berline J, Herrera R, Penaranda ME, Nakagawa M, Palefsky J. Inhibition of human papillomavirus type 16 E7 phosphorylation by the S100 MRP-8/14 protein complex. *J Virol* 2005; **2**: 1099–1112.
- 23 Xu TP, Liu XX, Xia R, Yin L, Kong R, Chen WM *et al*. SP1-induced upregulation of the long noncoding RNA TINCR regulates cell proliferation and apoptosis by affecting KLF2 mRNA stability in gastric cancer. *Oncogene* 2015; **45**: 5648–5661.
- 24 Garg M, Kanojia D, Okamoto R, Jain S, Madan V, Chien W *et al*. Laminin-5 $\gamma$ -2 (LAMC2) is highly expressed in anaplastic thyroid carcinoma and is associated with tumor progression, migration, and invasion by modulating signaling of EGFR. *J Clin Endocrinol Metab* 2014; **1**: E62–E72.



This work is licensed under a Creative Commons Attribution-NonCommercial-ShareAlike 4.0 International License. The images or other third party material in this article are included in the article's Creative Commons license, unless indicated otherwise in the credit line; if the material is not included under the Creative Commons license, users will need to obtain permission from the license holder to reproduce the material. To view a copy of this license, visit <http://creativecommons.org/licenses/by-nc-sa/4.0/>

© The Author(s) 2017

Supplementary Information accompanies this paper on the Oncogene website (<http://www.nature.com/onc>)